



HYDROGEN DESULFURIZATION OF NICKEL: THERMODYNAMICS AND KINETICS

William E. Frazier, Thu-Ha T. Mickle and Bruce A. Pregger
Air Vehicle and Crew Systems Technology Department (Code 6063)
NAVAL AIR WARFARE CENTER
AIRCRAFT DIVISION
P.O. Box 5152
Warminster, PA 18974-0591

1 NOVEMBER 1993

DTIC
ELECTED
JUL 27 1994
S G D

FINAL REPORT
Period Covering 1 January 1993 to 27 October 1993

Approved for Public Release; Distribution is Unlimited.

Prepared for
Air Vehicle and Crew Systems Technology Department (Code 60C)
NAVAL AIR WARFARE CENTER
AIRCRAFT DIVISION
P.O. Box 5152
Warminster, PA 18974-0591

94-23300

NOTICES

REPORT NUMBERING SYSTEM — The numbering of technical project reports issued by the Naval Air Warfare Center, Aircraft Division, Warminster is arranged for specific identification purposes. Each number consists of the Center acronym, the calendar year in which the number was assigned, the sequence number of the report within the specific calendar year, and the official 2-digit correspondence code of the Functional Department responsible for the report. For example: Report No. NAWCADWAR-92001-60 indicates the first Center report for the year 1992 and prepared by the Air Vehicle and Crew Systems Technology Department. The numerical codes are as follows:

CODE	OFFICE OR DEPARTMENT
00	Commanding Officer, NAWCADWAR
01	Technical Director, NAWCADWAR
05	Computer Department
10	AntiSubmarine Warfare Systems Department
20	Tactical Air Systems Department
30	Warfare Systems Analysis Department
50	Mission Avionics Technology Department
60	Air Vehicle & Crew Systems Technology Department
70	Systems & Software Technology Department
80	Engineering Support Group
90	Test & Evaluation Group

PRODUCT ENDORSEMENT — The discussion or instructions concerning commercial products herein do not constitute an endorsement by the Government nor do they convey or imply the license or right to use such products.

Reviewed By: J. W. Waldman _____

Date: 4/4/94

Branch Head

Reviewed By: J.S. Shaffer _____

Date: 4/5/94

Division Head

Reviewed By: T.E. Milhouse _____

Date: 4/15/94

Director/Deputy Director

REPORT DOCUMENTATION PAGE

Fcrn Approved
CMB No 0704-0188

Public reporting burden for this collection of information is estimated to average 1 hour per response, including the time for reviewing instructions, searching existing data sources, gathering and maintaining the data needed, and completing and reviewing the collection of information. Send comments regarding this burden estimate or any other aspect of this collection of information, including suggestions for reducing this burden, to Washington Headquarters Services Directorate for Information Operations and Reports, 1215 Jefferson Davis Highway, Suite 1204, Arlington, VA 22202-4302, and to the Office of Management and Budget, Paperwork Reduction Project (0704-0188), Washington, DC 20503.

NOMENCLATURE

\bar{v}	Average velocity of nickel atom in the gas phase
π	Pi
γ	Henrian activity coefficient of evaporating element
ΔG°	Gibb's Standard Free Energy of Formation
C	Concentration of sulfur
C_{eq}	Equilibrium concentration of nickel in the gas phase
C_o	Initial concentration of sulfur
D	Diffusion coefficient
d	Atomic diameter
dx/dt	Surface recession rate
h	Thickness of the nickel specimen
i, j	indices
J	Atomic flux
k	Boltzmann's constant
M, M_{wt}	Molecular weight
m	Average mass of an atom in the gas phase
P_{eq}	Equilibrium (saturation pressure) of nickel gas
Q	Activation energy for the diffusion of sulfur in nickel
R	Gas constant
T	Temperature
t	Time
X	Mole fraction of the evaporating element
x	Distance

Accesion For	
NTIS	CRA&I
DTIC	TAB
Unannounced	
Justification	
By	
Distribution /	
Availability Codes	
Dist	Avail and/or Special
A-1	

INTRODUCTION

Sulfur has been associated with the reduced environmental resistance of nickel-base superalloys [1,2]. The sulfur causes the protective aluminum oxide to spall and greatly reduces the life of coatings, e.g., thermal barrier coatings. Most of the nickel-base superalloys have bulk sulfur contents of less than 12 ppm; however, these alloys exhibit internal and external surface sulfur concentrations that can exceed 1,000 ppm [3,4]. If the surface sulfur is removed either mechanically or chemically, the surface sulfur concentration quickly returns to these high levels upon annealing. The sulfur diffuses to the surface against a high concentration gradient in apparent opposition to Fick's Laws.

The explanation, in part, is that sulfur reduces nickel's surface energy and that the chemical potential of sulfur on the surface of nickel is significantly less than in its interior. Small amounts of elements such as S, C, N, O, and P which tend to segregate to surfaces can cause a profound change in surface energy [5,6,7]. These surface active elements are also known to affect the surface tension of other metals [6,8]. The presence of 0.07 wt.% nitrogen in liquid iron reduces its surface energy by nearly 15%. As little as 0.09 wt.% oxygen can lower the surface energy of liquid iron by nearly 30% [5], and 0.1 wt.% sulfur reduces iron's surface energy by nearly 50% [8].

Sulfur is an unusual element. It exhibits allotropes in its solid, gas, and liquid forms. In the solid form, it is found in the rhombohedral, monoclinic and amorphous phases with specific gravities of 2.07, 1.96, and 1.92 respectively. Sulfur is a low melting point element: it melts at 112.8°C (rhombohedral) and boils at 444.67°C. Figure 1 is a plot of the equilibrium partial pressure of sulfur as a function of temperature [9]. This would seem to indicate that by merely raising the temperature of a nickel specimen above the boiling point of sulfur one could readily remove sulfur by evaporation. The fact that sulfur does not behave in this manner indicates that it is not in its elemental form.

The sulfur effect in superalloys can be reduced either by reducing sulfur's mobility within the alloy or by actually removing the impurity from the part. The first method is used commercially. Reactive elements such as yttrium or hafnium are added to

the alloy as sulfur getters. The resulting sulfur compounds are too low in concentration to affect bulk mechanical properties, but sulfur is immobilized and cannot segregate to the surface. The second approach, which has a potential economic advantage over the first (alloying with reactive elements is expensive and difficult), involves reducing the bulk concentration of sulfur in as-cast parts to less than 1 ppm. Sulfur has been successfully removed from alloy surfaces by reaction with hydrogen gas at high temperatures [10]. Surface sulfur reacts to form gaseous hydrogen sulfide. Sulfur is known to concentrate on free surfaces and internal interfaces. This ensures a continuous replenishment from the bulk of the sample and concentrations below 1 ppm have been achieved.

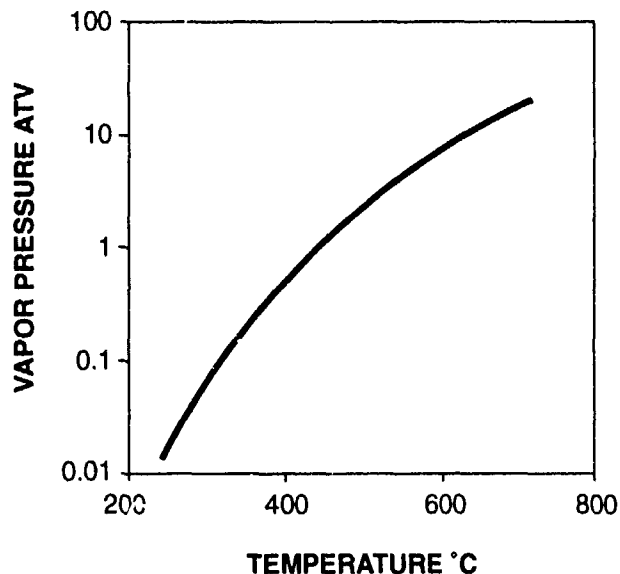


Figure 1. Vapor pressure of elemental sulfur as a function of temperature.

This paper examines the thermodynamics and kinetics of nickel desulfurization by hydrogen desulfurization and presents idealized models to quantitatively describe the process.

APPROACH

PHYSICAL MODEL

The physical model is a closed system: a furnace, nickel specimen, and an atmosphere of 100% H₂. The furnace is assumed to be much larger than the specimens. The nickel specimens are in the form of sheet and have a finite thickness ranging from 0.38 to 1.78 mm (15 to 70 mils). The length and width of the sheet is large enough with respect to its thickness to be considered infinite. The furnace is used to anneal the nickel specimens at 1200 and 1250°C and a pressure of one atmosphere. The temperatures were selected to be high enough to assure rapid sulfur removal but below the solution heat treatment temperature of today's superalloys in order to maintain the material's microstructure and properties.

THERMODYNAMIC MODEL

The initial sulfur concentration of the nickel specimen is assumed to be 10 ppm; the sulfur is taken to be in solid solution. The concentration of sulfur on the surface of the nickel specimen is assumed to be 1000 ppm, a typical value reported in the literature[3,4]. A monatomic, amorphous layer of Ni₃S₂ is assumed to exist on the surface of the nickel sheet. This is consistent with the following data: (i) elemental sulfur boils at temperatures exceeding 444.67°C, (ii) all the binary nickel-sulfur compounds are molten in this temperature regime, and (iii) sulfur is present in such low concentrations that only the nickel-rich compound Ni₃S₂ is compositionally stable.

Free energy data taken from the JANAF Thermochemical Tables [11] was used to assess the stability of the various nickel-sulfur compounds and those of H₂, H₂S, and HS. A linear regression analysis was used to generate equations for free energy as a function of temperature, Eq. 1. Equation constants are presented in Table 1.

$$\Delta G^\circ = A + BT \quad (1)$$

Table 1. Constants for the Free Energy of Formation of Various Sulfides at a Constant Sulfur Activity.

Compound	Temperature Range, °C	A (KJ/mol)	B (KJ/mol °K)
H ₂ S	900–2000	-181.02	0.0991
HS	900–2000	232.5	-0.1727
NiS	1100–2000	-212.35	0.0906
NiS ₂	1200–1800	-186.37	0.120
Ni ₃ S ₂	1000–2000	-240.81	0.0652
Ni ₃ S ₄	900–1100	-261.44	0.153

A plot of the free energies of formation for the various compounds considered is presented in Figure 2. The more negative the free energy of formation is for a particular compound, the more thermodynamically stable the compound. With the exception of NiS₂ (not stable at low sulfur levels), all of the nickel-sulfur compounds are inherently stable with respect to H₂. Conditions under which desulfurization can occur are discussed in the Results and Discussion section of this paper.

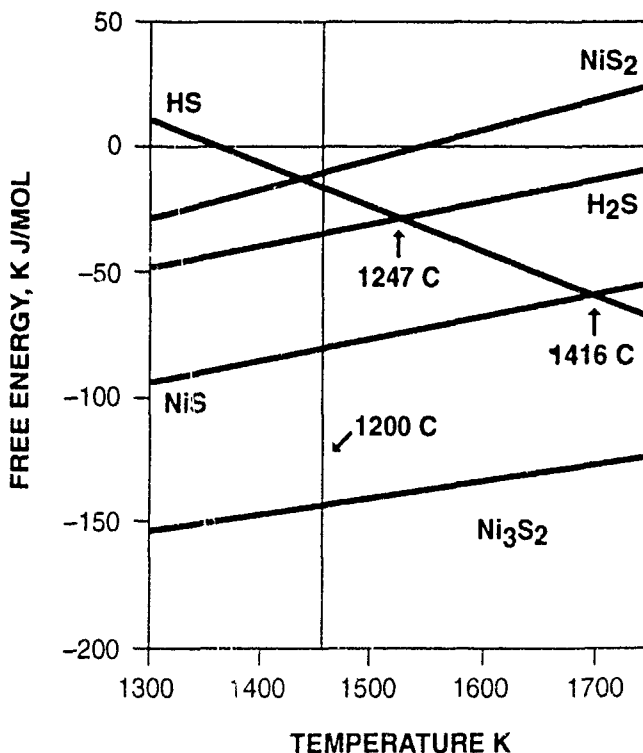


Figure 2. Gibb's free energies of formation for several compounds of sulfur.

KINETIC MODEL

At the elevated temperatures under consideration it is reasonable to assume that the reaction of hydrogen with Ni_3S_2 present on the specimen's surface is rapid. The continued elimination of sulfur in this manner requires that the sulfur in solid solution nickel diffuse to the specimen's surface. This solid state diffusion is then assumed to be the rate limiting step in the process.

In order to model the kinetics of the process, the physical model described previously has been adopted and the following additional conditions are imposed:

1. The elimination of sulfur is accomplished by the diffusion of sulfur outward to both sides of a plate of thickness, h . The length and width of the specimen is large enough with respect to thickness to be considered infinite.
2. The effective concentration of sulfur at the specimens surface is taken to be zero. In light of the empirical evidence indicating that the surface sulfur composition is approximately 1000 ppm [3,4], justification for this assumption is as follows. The surface sulfur is tied up as a monatomic layer of Ni_3S_2 not in solid solution and the chemical potential of sulfur in this form is believed to be extremely small.

The solution of the problem requires the application of Fick's second law, Eq. 2, and the following boundary conditions:

$$\begin{aligned} C &= C_0 \quad \text{for } 0 < x < h, \text{ at } t = 0 \\ C &= 0 \quad \text{for } x = h \text{ and } x = 0, \text{ at } t > 0 \end{aligned}$$

$$\frac{\partial C}{\partial t} = D \frac{\partial^2 C}{\partial x^2} \tag{2}$$

The value of the diffusion coefficient can be calculated using Equation 3 [10].

$$D = 1.4 \exp\left(\frac{-Q}{RT}\right) (\text{cm}^2/\text{s}) \tag{3}$$

where $Q = 218,600 \text{ (J)}$

$R = 8,314 \text{ (J/mol}^\circ\text{K)}$

$T = \text{Temperature } (\text{ }^\circ\text{K})$

The diffusivity of sulfur in a variety of metals is presented in Figure 3. The diffusion coefficient of sulfur in nickel at the temperatures of interest has values ranging from 2×10^{-9} to $4 \times 10^{-7} \text{ cm}^2/\text{s}$ [12]. The solution to equation 2 under the boundary conditions stated above has been worked out by other researchers [13]. The equation describing the compositional profile is presented in equation 4.

$$C(x,t) = \frac{4C_0}{\pi} \sum_{j=0}^{\infty} \frac{1}{2j+1} \sin \frac{(2j+1)\pi x}{h} \exp \left[-\frac{(2j+1)^2 \pi^2}{h^2} \cdot Dt \right] \quad (4)$$

The equation for the average composition of the specimen Eq. 5 is obtained by integrating equation 4 over the specimen thickness.

$$\frac{\bar{C} - C_s}{C_o - C_s} = \frac{8}{\pi^2} \sum_{n=0}^{\infty} \frac{1}{(2n+1)^2} \exp \left[-\frac{(2n+1)^2 \pi^2}{h^2} \cdot Dt \right] \quad (5)$$

SURFACE RECESSION RATE

The rate of nickel loss, the rate at which the specimen's surface recedes during thermal treatments may be calculated using equation 6. This problem may be modeled by assuming either diffusion controlled kinetics or the Langmuir-Kundsen model based on ideal gas law kinetics.

$$\frac{dx}{dt} = -\frac{JM_{wt}}{\rho} \quad (6)$$

Diffusion Controlled Model:

If the flux of nickel from the specimen's surface into the hydrogen gas environment is assumed to be diffusion controlled, then the flux may be modeled using equation 7. The application of this equation is difficult because the diffusion coefficient of nickel in hydrogen gas is unknown, the concentration profile of nickel is also unknown, and the atomic flux is a function of both position and time.

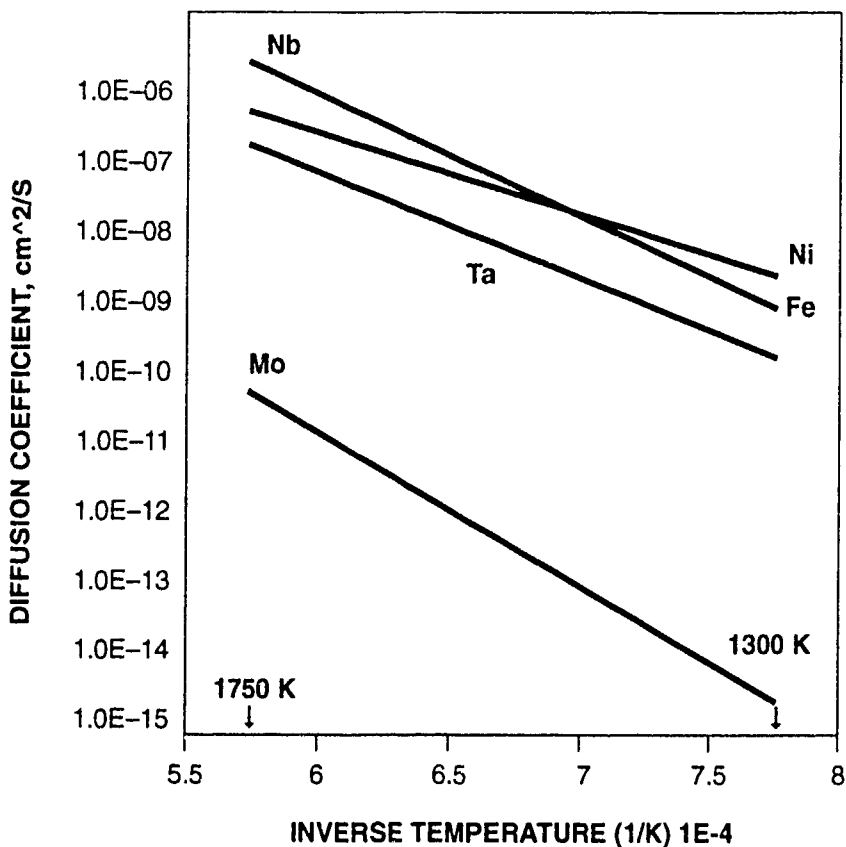


Figure 3. The diffusion coefficient of sulfur in several elements.

$$J = -D \left(\frac{C_{eq} - C_i}{\sqrt{\pi D t}} \exp \left(\frac{-x^2}{4 D t} \right) \right) \quad (7)$$

In order to estimate the diffusion coefficient, the semi-empirical equation 8 [14] was used.

$$D = \frac{3}{8} \sqrt{\frac{\pi k T}{2m}} \frac{1}{n \pi d^2} \quad (8)$$

where the m is

$$m = \frac{m_H m_{Ni}}{m_H + m_{Ni}} \quad (9)$$

and the average atomic diameter is

$$d = \frac{d_H + d_{Ni}}{2} \quad (10)$$

and n is the number of atoms per unit volume

$$n = \frac{P}{kT} \quad (11)$$

In order to estimate the concentration of nickel at the specimen's surface, equilibrium between solid nickel and its vapor is assumed. The further assumption of ideal gas behavior permits the calculation of concentration of nickel using the ideal gas law, Eq. 12.

$$C_{eq} = \frac{P_{eq}}{RT} \quad (12)$$

Modified Langmuir-Kundsen Model (based on ideal gas laws)

More straight-forward approach is to assume ideal gas law kinetics. The flux of atoms through a unit area may be calculated using equation 13 [14].

$$J = \frac{n\bar{v}}{4} \quad (13)$$

The average velocity of the atoms is calculated using equation 14 [14].

$$\bar{v} = \sqrt{\frac{8kT}{\pi m}} \quad (14)$$

Rearrangement of the preceding two equations and equation 6 enables one to calculate the rate of weight loss per unit area. In a vacuum, the rate of weight loss is proportional to equilibrium saturation pressure of the material. Conversely, the rate at which the material condenses onto the specimen's surface is proportional to the partial pressure of material in the gas phase. The net rate of weight loss per unit area is the difference of these two rates [15]. The rate at which the specimen's surface recedes during thermal treatments may be calculated by dividing weight loss (with units of g/cm²s) by density, equation 15.

$$\frac{dx}{dt} = (P_{eq} - P) \frac{X_1 \gamma_1}{\rho} \sqrt{\frac{M_{wt}}{2\pi RT}} \quad (15)$$

Assuming ideal behavior, the recession rate of nickel as a function of the partial pressure of nickel annealed at 1200°C is graphically portrayed in Figure 4. Recession rate approaches zero near the equilibrium vapor pressure of nickel, viz.,

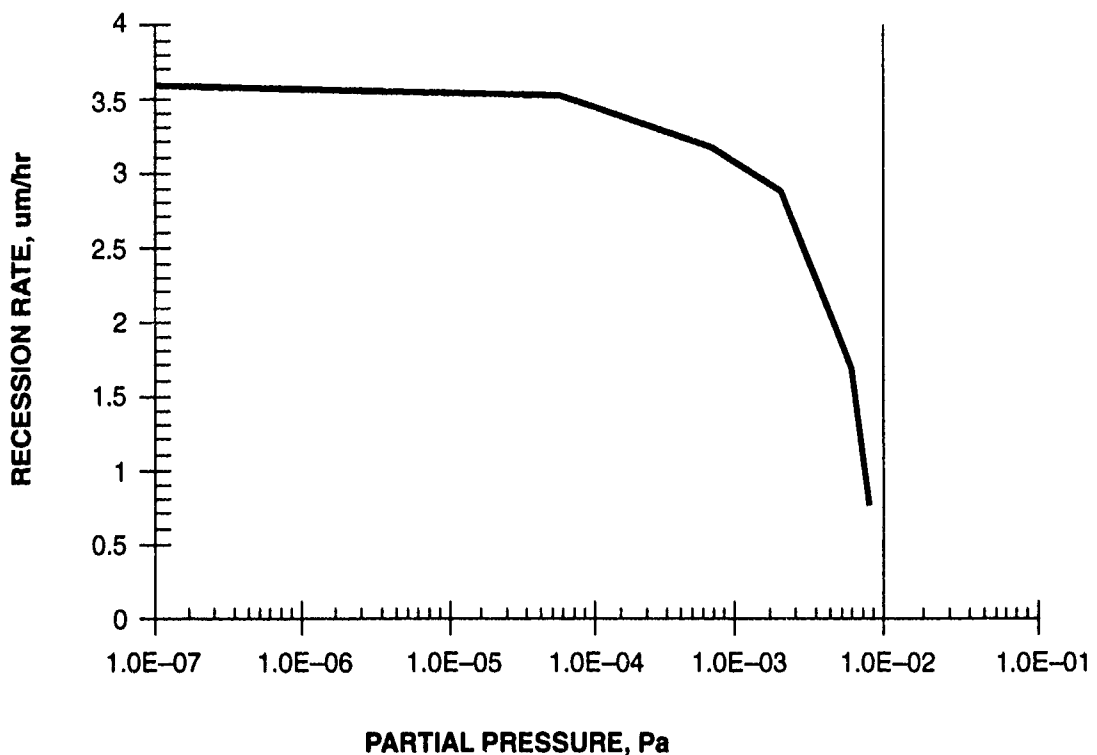


Figure 4. Calculated recession rate of a nickel specimen versus the environmental partial pressure of nickel.

0.01 Pa. Nickel's recession rate increases rapidly from zero at 0.01 Pa to $3.18 \mu\text{m/hr}$. at a partial pressure of 0.001, and quickly levels off to a pressure independent value of $3.53 \mu\text{m/hr}$.

RESULTS AND DISCUSSION

THERMODYNAMIC

The question to be addressed is under what conditions can H_2 reduce Ni_3S_2 ? In order for hydrogen to react with Ni_3S_2 , it must do so in accordance with equations 16 and 17, thus forming H_2S and HS as reaction products.



and



The equilibrium partial pressures of H_2S , HS, and H_2 were calculated from the equilibrium constants obtained for reactions. These equilibrium partial pressures are plotted as a function of temperature in Figure 5.

Application of LeChatlier's Principle suggest that reducing the partial pressure of the reaction products below their equilibrium value should drive the reaction towards completion. Although the equilibrium partial pressures of H_2S and HS are very small, approximately 0.01 atmospheres, the total quantity of sulfur available in the nickel specimen is also very small; consequently, our calculations indicate that the reaction will take place and equilibrium partial pressures are not likely to be achieved.

KINETIC

Equations 4 and 5 were derived for the desulfurization of nickel assuming that the diffusion of sulfur in nickel was the rate limiting step. Numerical answers to these equations were obtained using Math Cad 4.0 and are presented in Figures 6,7,8. Figures 6 and 7 show the position dependent concentration of sulfur in a 0.178 cm and 0.038 cm (70 and 30 mil) thick specimen hydrogen annealed at 1200°C . After four hours, the concentration of sulfur at the center of the thinner specimen has been reduced by 40%; whereas, the concentration of sulfur at the center of the

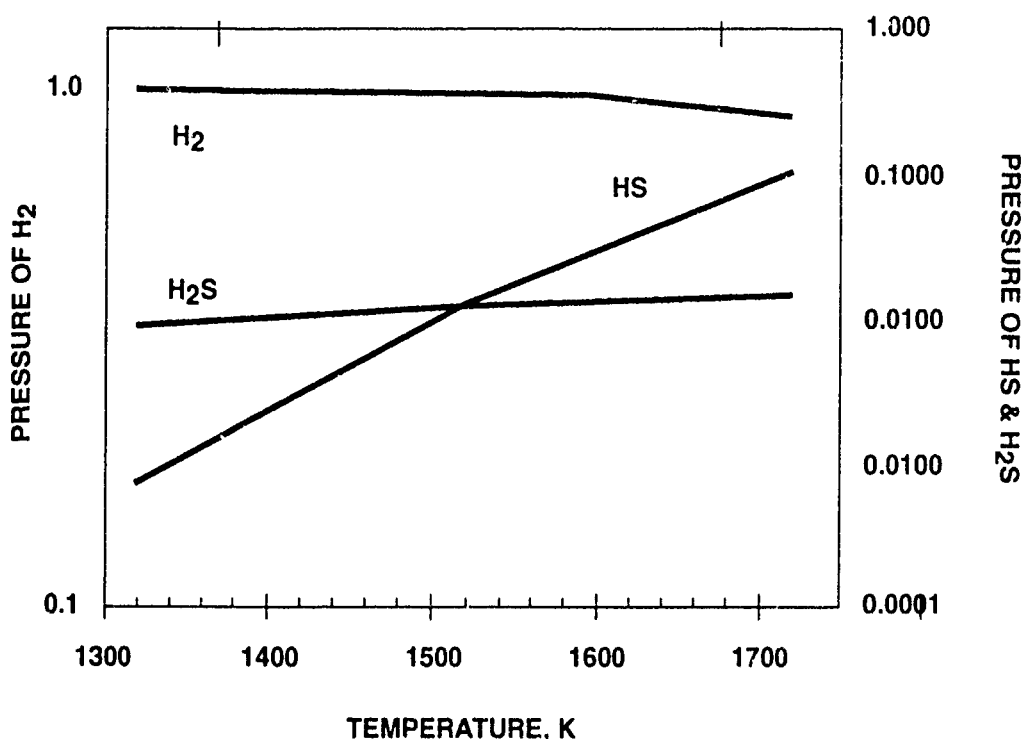


Figure 5. The calculated equilibrium partial pressures of HS, H_2S , and H_2 during the desulfurization of nickel.

thicker specimen remains virtually unchanged. In fact, it takes almost 24 hours for the concentration of sulfur at the center of the thicker specimen to be reduced by 40%.

While the compositional profiles shown in Figures 6 and 7 are important to our understanding of the desulfurization process, the average composition of the nickel sheet is more readily measured and therefore may be of more practical significance. Figure 8 show the calculated average composition of 0.038, 0.076, and 0.178cm (15, 30, and 70 mil) thick sheet annealed at 1200 and 1250°C. Clearly, both reducing the thickness and increasing the temperature enhance desulfurization.

The amount of sulfur removed from a 0.078cm (30 mil) thick specimen after 20 hours at 1250°C is an order of magnitude greater than at 1200°C. However, the amount of sulfur removed from a 0.178cm (70 mil) thick specimen after 20 hours at 1250°C is only twice as great as that removed at 1200°C. The nonlinear nature of

NAWCADWAR-93074-60

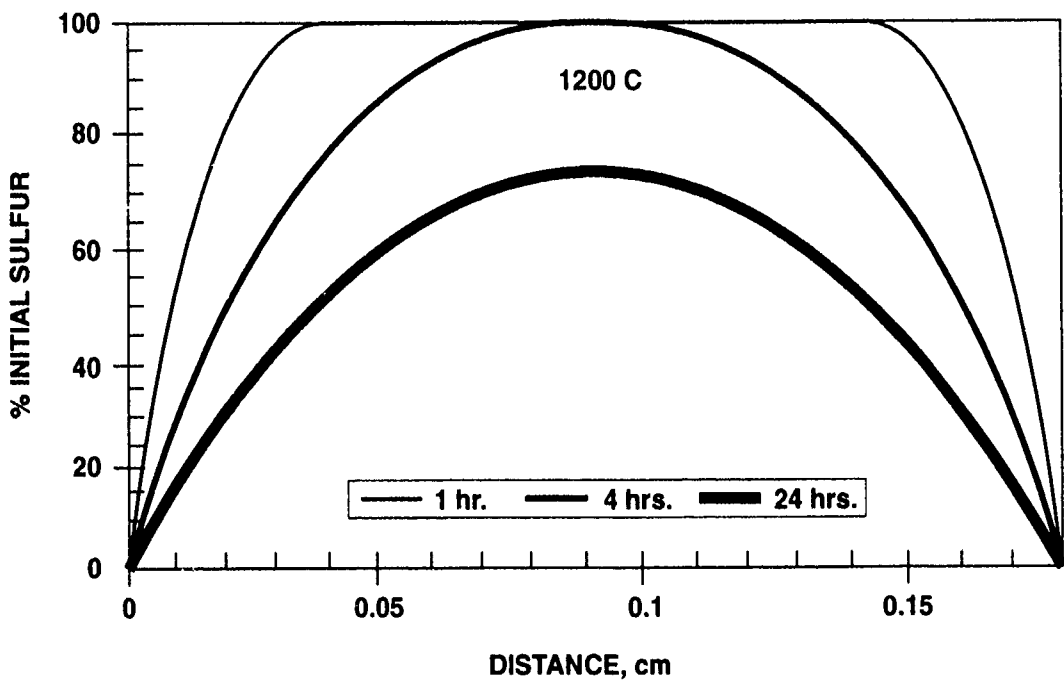


Figure 6. The position dependent concentration of sulfur in a 0.178cm (70 mil) thick specimen hydrogen annealed at 1200°C.

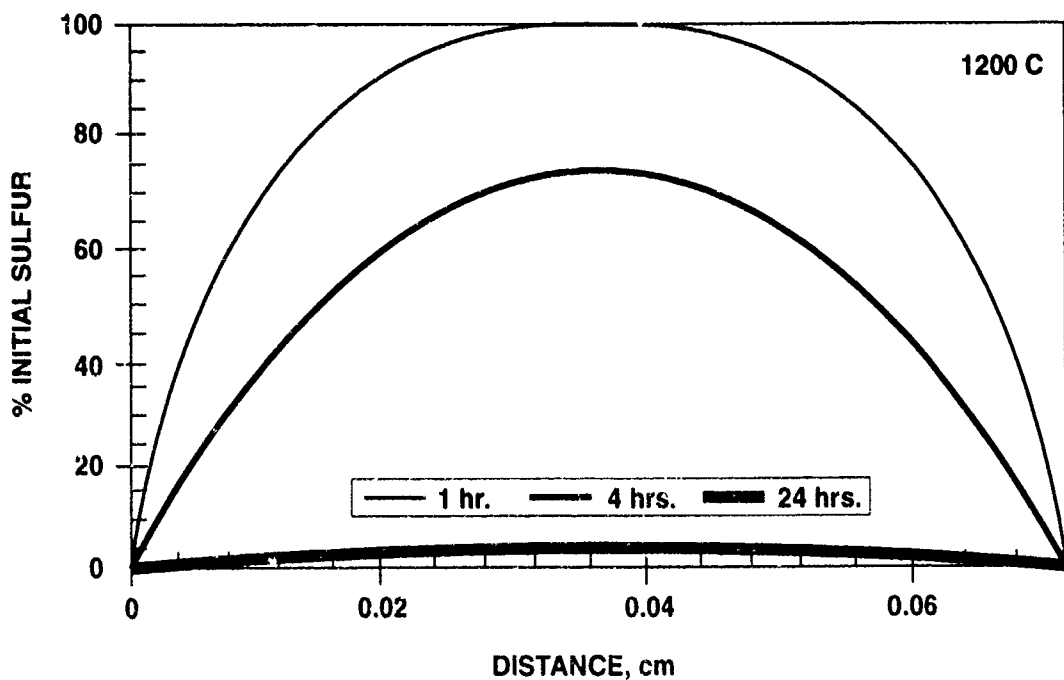


Figure 7. The position dependent concentration of sulfur in a 0.038cm (30mil) thick specimen hydrogen annealed at 1200°C.

desulfurization and the impact of annealing time, temperature, and specimen thickness on the amount of sulfur remaining after desulfurization is also clearly illustrated in Figure 8. As one would expect, increasing exposure time, increasing furnace temperature, and decreasing specimen size results in specimens with lower concentrations of sulfur.

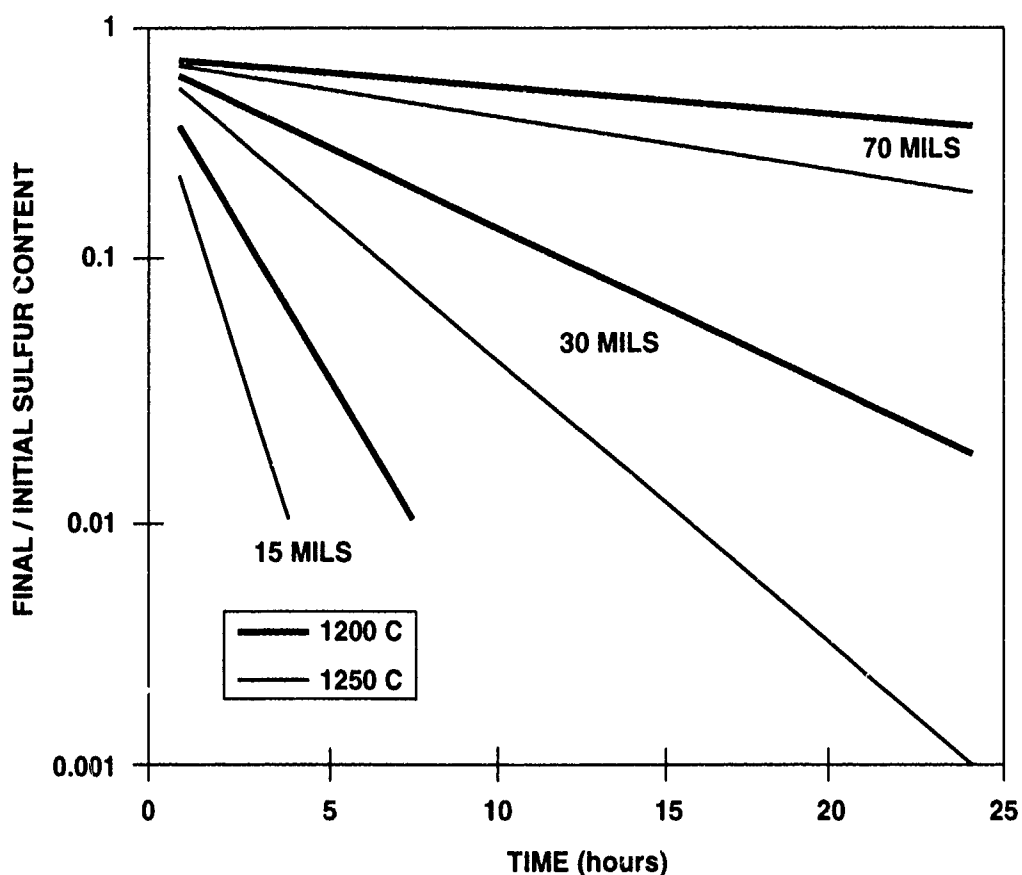


Figure 8. The calculated average composition of 0.038, 0.076, and 0.178cm (15, 30, and 70 mil) thick sheet annealed at 1200 and 1250°C.

SURFACE RECESSION

The loss of specimen mass during elevated temperature thermal treatments is of technological importance. The loss may be treated in terms of how rapidly the surface of the specimen recedes. Equations 6 through 11 constitute a diffusion

based model for the approximation of recession rate. The concentration of gaseous nickel at the specimen's surface and the diffusion coefficient of nickel in the gas are estimated. While a recession rate may be calculated, its value is highly dependent upon atomic flux and atomic flux is position and time dependent. The model also assumes that diffusion is the primary mass transport phenomenon responsible for nickel evaporation and neglects the effect of convective flow. Convective flow would be expected to disturb the compositional gradient and alter the evaporation rate.

The modified Langmuir-Kundsen Model provides a more straight forward way of calculating recession rate. The recession rate of a nickel specimen annealed at 1200°C has been calculated to be $3.53\mu/\text{hr}$ assuming an environmental partial pressure of nickel equal to zero. As can be observed in Figure 4, recession rate is a strong function of the partial pressure of nickel near nickel's saturation partial pressure, but weakly dependent at very low partial pressures.

Table 2. The Calculated Recession Rate of Nickel at 1200°C.

Saturation Partial Pressure of Nickel, Pa	Calculated Recession Rate, μ/hr
0.01	3.53
0.02	7.07
0.03	10.6

Recession rate is strongly dependent upon the saturation partial pressure, and the saturation partial pressure is strongly dependent upon temperature.

Experimental verification of the models for the recession rate of nickel was undertaken. A sphere of pure nickel was annealed at 1200°C in an atmosphere of hydrogen for 30 hours. The mass and dimensions of the nickel sphere were recorded before and after annealing. Examination of the nickel sphere after annealing indicated uniform mass loss. The recession rate for pure nickel was measured to be $6.41\mu/\text{hr}$.

SUMMARY AND CONCLUSIONS

The thermodynamics of hydrogen desulfurization have been explored. Removal of sulfur from the nickel sheet is considered viable under non-equilibrium conditions. That is, the concentration of HS and H₂S must be kept low, much less than 0.01 atm. This condition is readily achieved in a large furnace or in a furnace with flowing hydrogen gas.

The assumption of diffusion controlled kinetics results in pragmatic and technological limitations. Ninety nine percent of the sulfur can be removed in 24 hours from specimens 0.76 mm (30 mils) thick and less; however, only 75 percent of the sulfur is removed in a 1.78 mm (70 mil thick) specimen subject to the identical treatment.

A model for the diffusion controlled recession rate of nickel has been derived. Unfortunately, its utility is seriously limited by the sensitivity of atomic flux to position and time. The modified Langmuir-Kundsen Model is readily applicable using handbook data for the equilibrium saturation pressure of nickel.

REFERENCES

1. N. Srinivasan and Y.V.R.K. Prasad, "Influence of Sulfur on the Processing Map for Hot Working of Nickel," *Scripta Metallurgica et Materialia*. 27(1992), 309-312.
2. M.H. Lee and Y.M. Park, "Effect of Ce and Hf on the Segregation of Sulfur and the Anodic Polarization of Nickel," *Scripta Metallurgica et Materialia*. 28(1993), 1059-1063
3. J.L. Smialek, "The Effect of Sulfur Content on Al_2O_3 Scale Adhesion," M.J. Bennett and G.W. Lorimer ed. *Microscopy of Oxidation*. (The Institute of Metals, 1991), 258-270.
4. A.W. Funkenbusch, J.G. Smeggil, and N.S. Bornstein, "Reactive Element-Sulfur Interaction and Oxide Scale Adherence," *Metallurgical Transactions A*. 16A(1985), 1164-1165.
5. T. Iida and R.I.L. Guthrie, *The Physical Properties of Liquid Metals*. (NY, NY: Oxford Univ. Press, 1988).
6. United States Steel, *The Making, Shaping and Treating of Steel, Ninth Edition*. ed., H. E. McGannon, (Pittsburgh, PA: Herwick and Held, 1971).
7. E.D. Hondros and M.P. Seah, "Interfacial and Surface Microchemistry," Eds. R.W. Cahn and P. Haasen, *Physical Metallurgy*. (NY, NY: Elsevier, 1983), 855-931.
8. F.A. Halden and W.D. Kingery, *Journal of Physical Chemistry*. (59)(1955), 557.
9. R. Hultgren et al., *Selected Values of the Thermodynamic Properties of the Elements*. (Metals Park, OH: American Society for Metals, 1973).
10. B.K. Tubbs and J.L. Smialek, "Effect of Sulfur Removal on Scale Adhesion To PWA 1480," V. Srinivasan and K. Vedula ed. *Corrosion & Particle Erosion at High Temperatures*. (Warrendale, PA: TMS, 1989), 459-486.
11. JANAF *Thermochemical Tables*. Third Edition, American Chemical Society, American Institute of Physics for the National Bureau of Standards, (14)(1985).
12. CRC *Handbook of Chemistry and Physics*. ed., R.C. Weast and M.J. Astle, (Boca Raton, FL: CRC Press, 1982).
13. P.G. Shewmon, *Diffusion in Solids*. (NY, NY: McGraw-Hill, 1963).
14. J.P. Holman, *Thermodynamics*. (NY, NY: McGraw-Hill, 1974), 281-350.
15. R.D. Pehlke, *Unit Processes of Extractive Metallurgy*. (NY, NY: Elsevier, 1973)

DISTRIBUTION LIST
Report No. NAWCADWAR-93074-60

	No. of Copies
University of California Dept. of Materials Science Berkeley, CA, 94720 J. Morris, Jr., R. O. Richie.....	2
University of California Santa Barbara CA 93106 C. G. Levi	1
University of Pennsylvania School of Engineering and Applied Science 109 Town Building David Pope.....	1
United Technologies Research Center Silver Lane East Hartford, CT 06108 William Allen, Norm Bornstein, Denish Gupta.....	3
U.S. Air Force AFOSR/NE Bldg. 410 Bolling AFB Washington, DC 20332-6448 Dr. Allen H. Rosenstein	1
The Wichita State University Dept of Mechanical Engineering Wichita, KS 67208 Jorge E. Talia.....	1

DISTRIBUTION LIST
Report No. NAWCADWAR-93074-60

	No. of Copies
Temple University Dept. of Mechanical Engineering 12th & Norris St. Phila., PA 19122 Jim S.J. Chen	1
United Technologies Research Center East Hartford, Connecticut 06108 William P. Allen, D.N. Duhl	2
University of California Dept. of Mechanical Engineering Irvine, CA 92717 Enrique J. Lavernia	1
University of Wisconsin Department of Metallurgy and Mineral Engineering 1509 University Av. Madison, WI 53706 John H. Perepezko	1
Wayne State University 5050 Anthony Wayne Drive Detroit, MI 48202 John Benci	1
Worcester Polytechnic Institute 100 Institute Road Worchester MA 01609-2280 D. Apelian	1
Pratt and Whitney P.O. Box 109600 West Palm Beach, FL 33410-9600 B. H. Walker, R. Anderson	2
Pratt and Whitney 400 Main Street East Hartford, CT 06108 David Dahl, Don Parielle	2

DISTRIBUTION LIST
Report No. NAWCADWAR-93074-60

	No. of Copies
NAVAIRSYSCOM Naval Air System Command Washington, DC 20361-5140 R. A. Retta (AIR-51412),.....	1
Naval Air System Command Washington, DC 20361-5140 J. Jarrett (AIR-51412J),.....	1
Naval Industrial Resources Support Activity Bldg. 75-2 Naval Base Phila., PA 19112-5078 L. Plonsky (NAVIRSA-203)	1
Naval Industrial Resources Support Activity Bldg. 75-2 Naval Base Phila., PA 19112-5078 D. Fabry (NAVIRSA-204)	1
Naval Post Graduate School Mechanical Engineering Department Monterey, CA 93943 T. McNelly.....	1
Naval Research Laboratory Washington, DC 20375, Metallurgy	1
Northrop, Aircraft Division One Northrop Av. Hawthorne, CA 90250 S. P. Agrawal and G. R. Chanani.....	2
Office of Naval Research 800 Quincy St. Arlington, VA 22217-5000 S. Fishman Code 12, G. Yoder Code 11,	2
Rice University MEMF, P.O. Box 1892 Houston, TX 77251 Enrique Berrera	1

DISTRIBUTION LIST
Report No. NAWCADWAR-93074-60

	No. of Copies
Michigan Technological University Houghton, Michigan 49931 M. McKimpson	1
NASA Headquarters 600 Independence Av. Washington, DC 20546 N. Mayer, S. Vennesi.....	2
NASA Langley Research Center Hampton, VA 23365 A. Taylor, L. Blackburn	2
NASA Lewis Research Center Cleveland, OH 44135 James Smialek.....	1
National Bureau of Standards Gaithersburg, MD 20899 R. Shaffer, J. R. Manning	2
National Science Foundation Office of Science and Technology Centers Division 1800 G Street, Washington, DC 20550 L. W. Haworth	1
NAWCADWAR Warminster, PA, 18974-5000 Library, Code 8131 (2 Copies), W.E. Frazier, Code 6063 (15 Copies).....	17
Washington, DC 20361 J. Collins Air-5304, L. Sloter Air-931	2
NAWCADWAR Lakehurst, NJ 08733-5100 R. Celin (AV624-2173), R. Jablonski (AV624-2174), G. Fisher (SESD) (AV624-1179),	3
NAWCADWAR P.O. Box 7176 Trenton, NJ 08628-0176 F. Warvolis (PE34), A. Culbertson, R. Mahortor	3

DISTRIBUTION LIST
Report No. NAWCADWAR-93074-60

	No. of Copies
Innovare Inc., Airport Road Commonwealth Park 7277 Park Drive Bath, PA 18014 Al R. Austen	1
Lockheed Missiles and Space Co. Metallurgy Dept. 93-10/204 3251 Hanover St. Palo Alto CA 94304 R. Lewis and J. Wadworth	2
Marko Materials Inc. 144 Rangeway Rd. N. Billerica, MA 01862 R. Ray.....	1
Martin Marietta Laboratories 1450 South Rolling Rd. Baltimore, MD 21227-3898 J. Venables, K.S. Kumar	2
Massachusetts Institute of Technology 77 Massachusetts Av. Cambridge, MA 20139 J. Cornie	1
Metal Working News 201 King of Prussia Rd. Radnor, PA 19089 R. R. Irving	1
Metal Working Technology Inc. 1450 Scalp Avenue Johnstown, PA 15904 W. L. Otto	1
McDonnell Aircraft Co. Box 516 Saint Louis, MO 63166 K. K. Sankaran.....	1

DISTRIBUTION LIST
Report No. NAWCADWAR-93074-60

	No. of Copies
Drexel University Dept. of Materials Engineering 32nd and Chestnut St. Phila., PA 19104 M. J. Koczak.....	1
Elkem Development Center 200 Deer Run Road Sewickley, PA 15143 Deepak S. Madan	1
Garrett Auxiliary Power Division 2739 East Washington Street P.O. Box 5227 Phoenix, AZ 85010 C. McCormick.....	1
General Electric Aircraft Engines 1 Neumann Way Cincinnati, OH 45215 Ben Nagaraj, Jon Schaeffer, Wendy Murphy	3
Grumman Aerospace Corp. Bethpage, NY 11714 M. Donnellan, P. N. Adler	2
Howmet Corp 1500 South Warner St. Whitall, MI 49461-1895 Metallurgy.....	1
Idaho National Engineering Laboratory P.O. Box 1625 Idaho Falls, ID 83415 J. R. Knibloe.....	1
Inco Alloys International P.O. Box 1958 Huntington, WV 25720 J. deBarbadillo	1

DISTRIEUTION LIST
Report No. NAWCADWAR-93074-60

	No. of Copies
Air Force Wright Aeronautical Lab Wrigth Patterson AFB OH 45433 W. Griffith (MLTM) and J. Kleek ('WL/MLLM).....	2
Allied-Signal Corp. P.O. Box 1021R Morristown, NJ 07960 S.K. Das and P. Gilman	2
Allison Gas Turbine Division P.O. Box 420, Indianapolis, IN 4C206-0420 Heidi Mueller-Largent, Don Frasier	2
ARPA, 3701 North Fairfax Drive Arlington, VA 22203 William Barker, Robert Crowe, Benn Wilcox	3
BDM International, Inc. 4001 N. Fairfax Dr. #750 Arlington, VA 22203 P. A. Parrish	1
Boeing Commercial Airplane Seatle WA W. Quist	1
Center for Naval Analyses 4401 Front Ave., P.O. Box 16268 Alexandria, VA 22302-0268	1
Clemson University Dept. of Mechanical Engineering Riggs Hall, Clemson, SC 29634-0921 H.J. Rack	1
Defense Technical Information Center Bldg. #5, Cameron Station Bldg. 5, Alexandria, VA 22314 (Attn. Adminstrator)	2